Rheology of Rodlike Macromolecules in Semidilute Solutions

Sushant Jain and Claude Cohen*

School of Chemical Engineering, Cornell University, Ithaca, New York 14853.
Received October 21, 1980

ABSTRACT: We have extended the theory of Doi and Edwards for the steady-state shear stress and viscosity of semidilute solutions of rodlike molecules over the whole range of shear rates. This was done by including the quadrad term in the stress expression which they neglected. We have also considered the linear response of the model to oscillating shear flows. The theoretical predictions have been compared with available experimental data. Certain aspects of the theory, like the cubic dependence on the concentration of the zero-shear-rate viscosity, are well obeyed in a relatively high concentration regime (much closer to the liquid crystal transition than to dilute solution concentrations). The stress expression used by Doi and Edwards is that obtained by Bird and co-workers for *dilute* solutions. The viscosity obtained from the extended theory does not compare well with available experimental data unless the stress expression is modified by replacing the rotation diffusion coefficient D_{r0} in dilute solution by D_r, the rotation diffusion in semidilute solutions.

Introduction

Recently Doi and Edwards[1] proposed a model for the dynamics of rodlike macromolecules in semidilute solution. They consider a solution of thin rodlike macromolecules in a Newtonian fluid in the concentration range

$$1/L^3 \ll c \ll 1/dL^2 \tag{1}$$

where c is the number of rods per unit volume and d and L are the diameter and length of the rods with $L \gg d$. The conditions $c \gg 1/L^3$ establishes that the rods are "hindered" such that the free rotation of each rod is hampered by the presence of other rods in the vicinity; on the other hand, the condition $c \ll 1/dL^2$ indicates that actual collisions are still rare such that the rods are randomly oriented at thermodynamic equilibrium. The rotational motion of the rod occurs with a Brownian rotary diffusion coefficient $\tilde{D}_r$ while its translational Brownian motion is severely restricted to the direction along its axis due to the presence of the surrounding rods. Doi and Edwards[1] derive the following relationships between D_{r0} and D_r, the rotary diffusion coefficients in dilute and semidilute solutions, respectively:

$$D_r = \beta D_{r0}(cL^3)^{-2} \tag{2}$$

where β is some numerical factor expected to be of order unity. Under flow conditions, when the rods are not randomly oriented, the rotary diffusion coefficient $\tilde{D}_r$ is given by

$$\tilde{D}_r(\vec{u},[f]) = D_r\left[(4/\pi)\int d^2\vec{u}'\, f(\vec{u}',t)\sin(\vec{u}\vec{u}')\right]^{-2} \tag{3}$$

where $(\vec{u}\vec{u}')$ is the angle between the orientation vectors $\vec{u}$ and $\vec{u}'$ and $f(\vec{u},t)$ is the distribution of orientation.

The differential equation which governs the distribution function $f(\vec{u},t)$ may be written as

$$\partial f(\vec{u},t)/\partial t = L_u f(\vec{u},t) - L_u' f(\vec{u},t) \tag{4}$$

where

$$L_u f(\vec{u},t) \equiv \vec{\nabla}_u\cdot\tilde{D}_r\vec{\nabla}_u f(\vec{u},t) \qquad L_u' f(\vec{u},t) \equiv \vec{\nabla}_u\cdot\dot{\vec{u}} f(\vec{u},t) \tag{5}$$

with

$$\vec{\nabla}_u \equiv \vec{\delta}_r\frac{\partial}{\partial r} + \vec{\delta}_\theta\frac{1}{r}\frac{\partial}{\partial\theta} + \vec{\delta}_\phi\frac{1}{r\sin\theta}\frac{\partial}{\partial\phi} \tag{6}$$

for the spherical coordinates $r \geq 0$, $0 \leq \theta \leq \pi$, and $0 \leq \phi \leq 2\pi$. The first term on the right-hand side of eq 4 is due to the diffusive flux as shown in eq 5, and the second term represents the convective flux where $\dot{\vec{u}}(t)$ is the drift velocity given by[1]

$$\dot{\vec{u}} = \bar{\bar{g}}\cdot\vec{u} - (\vec{u}\cdot\bar{\bar{g}}\cdot\vec{u})\vec{u} \tag{7}$$

with $\bar{\bar{g}}$ representing the velocity gradient tensor of a homogeneous linear flow; i.e., $g_{ij} = \partial v_i/\partial x_j$.

To determine the rheological properties (or any other macroscopic property) of the solution, the governing idea is to average the microscopic stress tensor (or other property) over the distribution of orientation $f(\vec{u},t)$ obtained under the specific flow condition. To that end, Doi and Edwards use a shear stress expression identical with that developed by Bird and co-workers[2] for *dilute* solutions of rigid dumbbell macromolecules; namely

$$\sigma_{ij} = -3ckT\langle u_iu_j\rangle - \frac{ckT}{D_{r0}}\sum_{k,l}g_{kl}\langle u_ku_lu_iu_j\rangle - \eta_s(g_{ij}+g_{ji}) + p\delta_{ij} \tag{8}$$

Under steady simple shear flow conditions and at low shear rate, the quadrad term (second term on the right-hand side) is small for g small compared to D_{r0} and has been neglected by Doi and Edwards. In this paper we extend these results to high rates of shear by including the quadrad term and obtain the response of the model to small-amplitude oscillatory shear flows.

Equation 8 has been obtained for dilute solutions of rigid dumbbell macromolecules, neglecting hydrodynamic interaction between the beads.[2] It has been successful in the interpretation of the rheological data of dilute solutions of rigid rodlike macromolecules such as tobacco mosaic virus[3] based on the assumption that a rod can be modeled as consisting of evenly spaced frictional beads along the length of the rod.[4] The use of eq 8 for semidilute solution neglects not only the intramolecular hydrodynamic interaction between the beads of the same molecule but also the intermolecular hydrodynamic interaction between different molecules. Furthermore, the experimental results on semidilute solutions of rigid rods of Hermans,[5] Kiss and Porter,[6] and Berry and co-workers[7] show that the normalized shear viscosity curve (η/η_0 vs. g/D_r) falls on a master curve *independent* of concentration. Such a behavior is not satisfied by the stress expression of eq 8 unless D_{r0} in the quadrad term is substituted by D_r, the rotation diffusion in semidilute solutions, so that a more appropriate expression would be

$$\sigma_{ij} = -3ckT\langle u_iu_j\rangle - \frac{ckT}{D_r}\sum_{k,l}g_{kl}\langle u_ku_lu_iu_j\rangle - \eta_s(g_{ij}+g_{ji}) + p\delta_{ij} \tag{9}$$

There is no theoretical basis for using eq 8 or eq 9 for this system of "hindered" rods. We note, however, that Curtiss and Bird have recently derived, in a self-consistent manner, an analogous expression for a polymer melt;[8] a similar

0024-9297/81/2214-0759$01.25/0

analysis for rigid-rod solutions is needed but is beyond the scope of this paper.

Simple Shear Flow

Under steady simple shear flow conditions, eq 4 reduces to

$$L_u f_s(\vec{u}) = L_u' f_s(\vec{u}) \tag{10}$$

which may be explicitly written as[1]

$$\left(\frac{1}{\sin\theta}\frac{\partial}{\partial\theta}\sin\theta\frac{\partial}{\partial\theta} + \frac{1}{\sin^2\theta}\frac{\partial^2}{\partial\phi^2}\right) f_s = g/\bar{D}_r \Gamma f_s \tag{11}$$

where $\bar{D}_r$ is an effective shear-rate-dependent diffusion coefficient[1] and Γ is given by

$$\Gamma = \cos^2\theta\cos\phi\frac{\partial}{\partial\theta} - \cot\theta\sin\phi\frac{\partial}{\partial\phi} - 3\sin\theta\cos\theta\cos\phi \tag{12}$$

for a shear flow in the (1,3) plane. Equation 11 is solved formally by expanding f_s in spherical harmonics:

$$f_s(\theta,\phi) = \sum_{\substack{l=0 \\ l\ \text{even}}}^{\infty}\sum_{m=0}^{l}(b_{lm}|l,m) \tag{13}$$

where $|l,m)$ represents a linear combination of spherical harmonics. Substituting in eq 10 yields

$$l(l+1)b_{lm} - \bar{\gamma}\sum_{\substack{l'=2 \\ l'\ \text{even}}}^{\infty}\sum_{m'=0}^{l'}(l,m|\Gamma|l',m')b_{l'm'} = \bar{\gamma}(lm|\Gamma|00)b_{00} \tag{14}$$

with $\bar{\gamma} = g/\bar{D}_r$ and where we have used the orthogonality relation of spherical harmonics. The matrix elements $(lm|\Gamma|l'm')$ can be calculated by using the recurrence relations of the harmonics. Equation 14 represents then a set of coupled linear algebraic equations in b_{lm} which may be determined by truncating the infinite series at a suitable l_{max}. We have taken values of l_{max} between 12 and 28, depending on the value of the shear rate; the higher the shear rate, the larger l_{max} must be for proper convergence. For a simple shear flow in the (1,3) plane, with $g_{13} \equiv g$, eq 8 for the stress expression reduces to

$$\sigma_{13} = -3ckT\langle u_1u_3\rangle - \frac{ckT}{D_{r0}}g\langle u_1u_3u_1u_3\rangle - \eta_s g \tag{15}$$

where it can be shown that

$$\langle u_1u_3\rangle = (4\pi/15)^{1/2}b_{21} \tag{16}$$

and

$$\langle u_1u_3u_1u_3\rangle = \frac{1}{14}\left(\frac{16\pi}{15}\right)^{1/2}\left(\left(\frac{4}{3}\right)^{1/2}b_{42} + b_{22}\right) + \frac{(4\pi)^{1/2}}{15}b_{00} + \frac{1}{42}\left(\frac{16\pi}{5}\right)^{1/2}b_{20} - \frac{1}{70}\left(\frac{256\pi}{9}\right)^{1/2}b_{40} \tag{17}$$

Equation 15 can then be rewritten, using eq 2, 16, and 17, as

$$-\frac{\sigma_{13}}{ckT} = 3\left(\frac{4\pi}{15}\right)^{1/2}b_{21} + \frac{g}{D_r}\beta(cL^3)^{-2}\left\{\frac{1}{14}\left(\frac{16\pi}{15}\right)^{1/2}\left(\left(\frac{4}{3}\right)^{1/2}b_{42} + b_{22}\right) + \frac{(4\pi)^{1/2}}{15}b_{00} + \frac{1}{42}\left(\frac{16\pi}{5}\right)^{1/2}b_{20} - \frac{1}{70}\left(\frac{256\pi}{9}\right)^{1/2}b_{40}\right\} + \eta_s g \tag{18}$$

From the definition of the shear viscosity

$$\eta(g) = \sigma_{13}/g \tag{19}$$

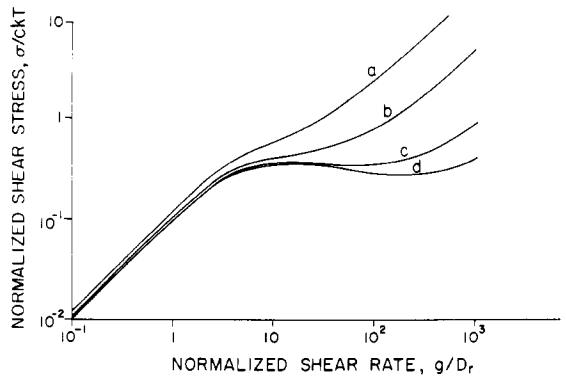

Figure 1. Plots of normalized shear stress vs. normalized shear rate calculated from eq 8 with $\beta = 1$: (a) $cL^3 = 3$, $\beta(cL^3)^{-2} = 1.1 \times 10^{-1}$; (b) $cL^3 = 5$, $\beta(cL^3)^{-2} = 4 \times 10^{-2}$; (c) $cL^3 = 10$, $\beta(cL^3)^{-2} = 1 \times 10^{-2}$; (d) $cL^3 = 15$, $\beta(cL^3)^{-2} = 4.4 \times 10^{-3}$.

the normalized shear viscosity, $\eta(g)/\eta(0)$, may then also be calculated.

Numerically calculated values of b_{lm} from eq 14 have been used to compute $\sigma_{13}(g)$ and $\eta(g)/\eta(0)$ using eq 18 and 19. Figure 1 shows plots of nondimensional shear stress, σ_{13}/ckT vs. nondimensionalized shear rate, $\gamma = g/D_r$. At low shear rates and above a certain concentration, only the dyad term is important and since it depends only on γ, the curves follow initially the same straight line (e.g., curves c and d at low g/D_r). This is the regime previously examined by Doi and Edwards. As the quadrad term increases with shear rate, the curves split for increasing shear rates, depending on the value of cL^3. Doi and Edwards[1] conjectured a sigmoidal shape for the shear stress vs. shear rate curve and discussed the associated flow instability. As seen in Figure 1, the shear stress does indeed go through a maximum and a minimum when the quadrad term is taken into account and when $\beta(cL^3)^{-2}$ is below a certain value ($\sim 10^{-2}$). This anomalous behavior is therefore predicted only if the solution is sufficiently concentrated. This behavior is not observed experimentally at any concentration in the isotropic phase mainly because, as we shall see later, the magnitude of β is much higher than was originally assumed by Doi and Edwards. One possible explanation for this discrepancy is that eq 2 has been obtained based on the assumption that the jump rotation frequency of a test rod is governed by the time it takes the rod hindering the test rod to diffuse a distance L along its length. That time could be much shorter since the hindering rod may not have to diffuse along a whole length L before freeing the test rod (see Discussion and Conclusion).

Figure 2 shows predicted graphs of viscosity vs. shear rate plotted in nondimensional form. Here again, all the curves can be represented by one master curve up to a certain value in shear rate ($\sim\gamma = 6$). For higher shear rates, however, the curves split due to the predominance of the quadrad term. It is also predicted that with increasing concentration the viscosity of the solution falls off more rapidly with increasing shear rate. The solution has one characteristic relaxation time $\bar{\lambda}$ (defined as $1/6\bar{D}_r$) which has a zero-shear-rate value given by

$$\lambda = 1/6D_r = (cL^3)^2/6\beta D_{r0} \tag{20}$$

and thus varies as the square of the concentration.

Oscillatory Shear Flow

We shall consider here the response of the model to an oscillating shear field of small amplitude. The imposed

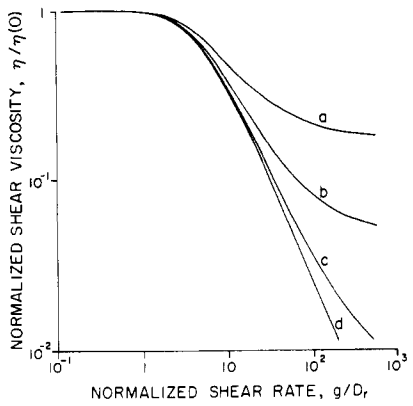

Figure 2. Plots of normalized shear viscosity vs. normalized shear rate: (a) $cL^3 = 3$, $\beta(cL^3)^{-2} = 1.1 \times 10^{-1}$; (b) $cL^3 = 5$, $\beta(cL^3)^{-2} = 4 \times 10^{-2}$; (c) $cL^3 = 10$, $\beta(cL^3)^{-2} = 1 \times 10^{-2}$; (d) as calculated by Doi and Edwards, neglecting the quartic term in eq 8.

shear field is again taken in the (1,3) plane and its only nonzero component is given by

$$g_{13}(t) = g(t) = g_0(e^{i\omega t} + e^{-i\omega t}) \tag{21}$$

where $g_{13}(t)$ and g_0 are both real. To solve for the distribution function in eq 4 under the flow condition of eq 21, $f(\vec{u},t)$ is again expanded in terms of spherical harmonics as

$$f(\vec{u},t) = \sum_{\substack{l=0 \\ l \text{ even}}}^{\infty} \sum_{m=0}^{l} (b_{lm}(t)|l,m) \tag{22}$$

where, due to the sinusoidal nature of the imposed shear rate, the coefficients $b_{lm}(t)$ are postulated to be of the form

$$b_{lm}(t) = \sum_{\alpha=-\infty}^{\infty} b_{lm}{}^{\alpha} e^{i\alpha\omega t} \tag{23}$$

Substituting for $f(\vec{u},t)$ from eq 22 and simplifying gives

$$\vec{\nabla}_u \cdot \bar{D}_r \vec{\nabla}_u [(b_{lm}(t)|l,m)] = \dot{b}_{lm}(t) + g(t) \sum_{\substack{l'=0 \\ l' \text{ even}}}^{\infty} \sum_{m'=0}^{l'} (l,m|\Gamma|l',m')b_{l'm'}(t) \tag{24}$$

The left-hand side of eq 24 is a highly nonlinear expression because of $\bar{D}_r(\vec{u},[f(\vec{u},t)])$. Again, as in the case of steady shear flow,[1] a diffusion coefficient, $\bar{D}_r$, averaged over orientations, is defined by

$$(\bar{D}_r)^{-1/2} = \langle \bar{D}_r^{-1/2} \rangle = D_r^{-1/2} \frac{4}{\pi} \int d^2\vec{u}\, d^2\vec{u}'\, f(\vec{u},t) f(\vec{u}',t) \sin(\vec{u}\vec{u}') \tag{25}$$

where

$$\bar{D}_r = D_r Q(\bar{\gamma})^{-1/2} \tag{26}$$

with

$$Q(\bar{\gamma}) \equiv \frac{4}{\pi} \int d^2\vec{u}\, d^2\vec{u}'\, f(\vec{u},t) f(\vec{u}',t) \sin(\vec{u}\vec{u}') \tag{27}$$

and

$$\bar{\gamma}(t) = g(t)/\bar{D}_r(t) \tag{28}$$

Equation 24 can then be rewritten as

$$\vec{\nabla}_u{}^2[(b_{lm}(t)|l,m)] = \left(\frac{1}{\bar{D}_r(t)}\right)\dot{b}_{lm}(t) + \frac{g(t)}{\bar{D}_r(t)} \sum_{\substack{l'=0 \\ l' \text{ even}}}^{\infty} \sum_{m'=0}^{l'} (l,m|\Gamma|l',m')b_{l'm'} \tag{29}$$

After substitution for $g(t)$ and $b_{lm}(t)$ from eq 21 and 23, we arrive, using properties of spherical harmonics and some simplifications, at

$$l(l+1) \sum_{\alpha=-\infty}^{\infty} b_{lm}{}^{\alpha} e^{i\alpha\omega t} - \frac{1}{\bar{D}_r(t)} \sum_{\alpha=-\infty}^{\infty} b_{lm}{}^{\alpha} i\alpha\omega e^{i\alpha\omega t} - \frac{g_0}{\bar{D}_r(t)} \sum_{l'} \sum_{m'} \sum_{\alpha=-\infty}^{\infty} A_{lml'm'} b_{l'm'}{}^{\alpha-1} e^{i\alpha\omega t} - \frac{g_0}{\bar{D}_r(t)} \sum_{l'} \sum_{m'} \sum_{\alpha=-\infty}^{\infty} A_{lml'm'} b_{l'm'}{}^{\alpha+1} e^{i\alpha\omega t} = \frac{g_0}{\bar{D}_r(t)} (e^{i\omega t} + e^{-i\omega t}) A_{lm00} b_{00} \tag{30}$$

$\bar{D}_r(t)$ is given by eq 26, with $Q(\bar{\gamma})$ expressed in terms of the coefficients $b_{lm}(t)$, by

$$Q(\bar{\gamma}) = 1 - 8\pi \sum_{\substack{l=2 \\ l \text{ even}}}^{\infty} \sum_{m=0}^{l} \left(\frac{l-1}{l+2}\right)\left[\frac{(l-3)!!}{l!!}\right](b_{lm}(t))^2 \tag{31}$$

It can be seen then that $\bar{D}_r(t)$ is a nonlinear function of time. However, under the simplifying assumptions that the imposed dimensionless amplitude $g_0/|\bar{D}_r(t)|$ of the oscillatory shear rate is small, we can investigate the linear response of the model.

In the limit of zero frequency, eq 23 gives

$$b_{lm} = \sum_{\alpha=1}^{\infty} (b_{lm}{}^{\alpha} + b_{lm}{}^{-\alpha}) + b_{lm}{}^{0} \tag{32}$$

where the b_{lm}'s are the coefficients for steady shear flow previously evaluated. From the solution of that problem, we know that the b_{lm}'s are at least proportional to $g_0/\bar{D}_r$ and since the contribution to b_{lm} from each $b_{lm}{}^{\alpha}$ is additive, each $b_{lm}{}^{\alpha}$ must also vary at least like $g_0/|\bar{D}_r(t)|$. Furthermore, the amplitude of each $b_{lm}(t)$ is determined by that of $b_{lm}{}^{\alpha}$'s. Hence, it can be seen in eq 31 that the amplitude of the terms under the summation sign varies at least like $[g_0/|\bar{D}_r(t)|]^2$. Under the linearity assumption, neglecting all nonlinear effects with amplitude of order $[g_0/|\bar{D}_r(t)|]^2$ and higher, eq 31 reduces to

$$Q(\bar{\gamma}) \simeq 1 \tag{33}$$

and eq 26 then gives

$$\bar{D}_r(t) \simeq D_r \tag{34}$$

With the above simplification, eq 30 can be easily solved by equating the coefficients of equal powers of $e^{i\omega t}$ to yield the desired $b_{lm}{}^{\alpha}$'s. The only contributions in the stress expression relevant to us here come from $b_{21}{}^{1}$, $b_{21}{}^{-1}$, and b_{00}, and we find for the stress

$$\frac{\sigma_{13} - \sigma_s}{ckT} = 2\,\mathrm{Re}\left[\frac{\frac{3}{5}(g_0\lambda)e^{i\omega t}}{(1 - i\omega\lambda)}\right] + \frac{2}{5}(g_0\lambda)\beta(cL^3)^{-2}(e^{i\omega t} + e^{-i\omega t}) \tag{35}$$

where σ_s is the solvent contribution and $\lambda = 1/6D_r$.

For a sinusoidal simple shear rate, the complex viscosity η^* is defined by the relations

$$\sigma(t) = \mathrm{Re}\,[\eta^* g(t)] \qquad \eta^* \equiv \eta' - i\eta'' \tag{36}$$

Therefore, using eq 35 and 36 gives

$$\eta^* - \eta_s = ckT\lambda\left\{\left[\frac{3}{5}\frac{1}{1 + (\lambda\omega)^2} + \frac{2}{5}\beta(cL^3)^{-2}\right] - i\frac{3}{5}\frac{(\lambda\omega)}{1 + (\lambda\omega)^2}\right\} \tag{37}$$

Hence

$$\eta' - \eta_s = ckT\lambda\left[\frac{3}{5}\frac{1}{1+(\lambda\omega)^2} + \frac{2}{5}\beta(cL^3)^{-2}\right] \quad (38)$$

and

$$\eta'' = ckT\left[\frac{3}{5}\frac{(\lambda\omega)}{1+(\lambda\omega)^2}\right] \quad (39)$$

Figure 3 shows plots of the normalized in-phase component of the viscosity $(\eta' - \eta_s)/(\eta'(0) - \eta_s)$ vs. the normalized frequency $(\lambda\omega)$. Note that for $\beta(cL^3)^{-2} = 1$, eq 37 reduces to the dilute-solution results of Kirkwood and Plock[9]

$$\eta^*_{dil} - \eta_s = ckT\lambda\left\{\left(1 - \frac{3}{5}\frac{(\lambda\omega)^2}{1+(\lambda\omega)^2}\right) - i\frac{3}{5}\frac{(\lambda\omega)}{1+(\lambda\omega)^2}\right\} \quad (40)$$

This is to be expected since in this case both the stress expression and the distribution functions become identical with those of dilute solutions with D_{r0} replaced by D_r. This would also be the result from the stress as expressed in eq 9.

Comparison with Experimental Data

We have found no available experimental data in the range of concentration specified by eq 1 for which the original theory was developed.[1] The concentration that comes nearest to fulfilling this requirement is a 1% PBLG [poly(γ-benzyl L-glutamate)] of molecular weight 2.75×10^5 in *m*-cresol examined by Hermans.[5] For this case, $cL^3 = 142$, whereas $L/d = 120$ based on the length and diameter measurements of Doty et al.[10] The results of the model deviate markedly from the experimental results at this concentration. Several aspects of the model are, however, well obeyed by the experimental results at *higher* concentrations; and with the modified stress expression of eq 9, the experimental shear viscosity curves (η vs. g/D_r) of Hermans,[5] Kiss and Porter,[6] and Berry and co-workers[7] on several rodlike macromolecules follow the theoretical predictions up to $g/D_r \simeq 25$. We now turn to these aspects of the model.

Zero-Shear-Rate Viscosity. Figure 4 shows plots of zero-shear-rate viscosity, $\eta(0)$, vs. c for three different molecular weights examined by Hermans.[5] Most of the data for the intermediate molecular weight, 2.7×10^5, and a few of the data points (at the high-concentration end of the spectrum) for the other molecular weights show excellent agreement with the prediction of the model that $\eta(0)$ is proportional to c^3. This indicates a shifting of the concentration range of applicability of the theory to much higher concentrations. Turning to the magnitude of $\eta(0)$, one can show that the stress expression of eq 9 leads to the following expression for $\eta(0)$:

$$\frac{\eta(0)}{\eta_s} = \frac{ckT}{6\eta_s D_{r0}\beta(cL^3)^{-2}} + 1 \quad (41)$$

Equation 41 in conjunction with the linear portion of the curve for the intermediate molecular weight in Figure 4 gives[11]

$$\beta = 8.8 \times 10^4 \quad (42)$$

The large value of β obtained when D_{r0} is estimated by Kirkwood's formula[12] and the fact that the c^3 dependence of $\eta(0)$ is obeyed at these high concentrations suggest that the effect of the length of the rods on hindrance has been overestimated in the model. Postulating an "effective" length L_e which is much shorter for the rod than its actual length, one can define an effective length factor ϵ such that

$$L_e = \epsilon L \quad (43)$$

where

$$\beta(cL^3)^{-2} = (cL_e^3)^{-2} \quad (44)$$

Combining eq 42 and 44 gives $\epsilon = 0.15$.

To obtain more insight into the concentration range for the applicability of the model at these higher concentrations, we calculated L_e for the two other molecular weights plotted in Figure 4. We use eq 41, 43, 44 and the values of $\eta(0)$ in the concentration regime where the $\eta(0)$ vs. c^3 relationship is obeyed (e.g., 6 wt % for $M = 2.2 \times 10^5$ and 4.7 wt % for $M = 3.42 \times 10^5$) to determine ϵ. Table I lists cL^3, cL_e^3, and ϵ obtained for the three different molecular weights considered. ϵ is found to be practically constant for the three molecular weights. By examining the cL_e^3 values obtained and Figure 4, we find that the $\eta(0)$ vs. c^3 relationship is obeyed for $cL_e^3 \gtrsim 1.5$ and up to almost the

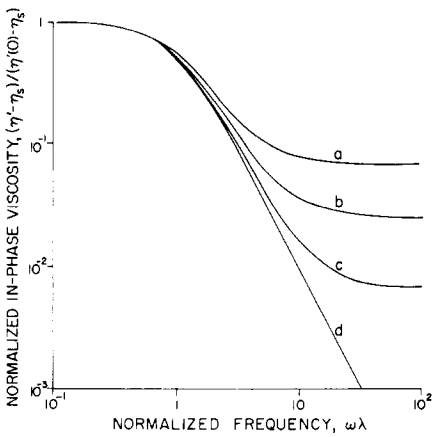

Figure 3. Plots of normalized in-phase viscosity vs. normalized frequency calculated from eq 38 with $\beta = 1$: (a) $cL^3 = 3$, $\beta(cL^3)^{-2} = 1.1 \times 10^{-1}$; (b) $cL^3 = 5$, $\beta(cL^3)^{-2} = 4 \times 10^{-2}$; (c) $cL^3 = 10$, $\beta(cL^3)^{-2} = 1 \times 10^{-2}$; (d) neglecting the second term on the right-hand side of eq 38.

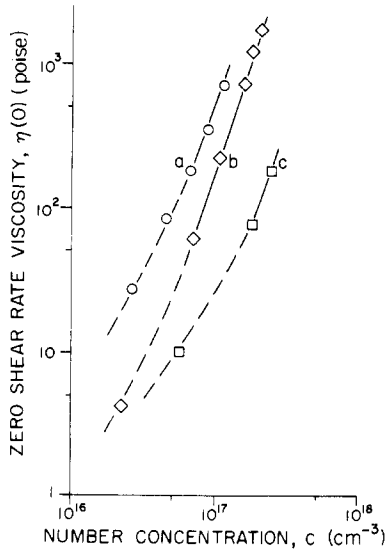

Figure 4. Plots of zero-shear-rate viscosity vs. number concentration for PBLG/*m*-cresol from ref 5 for three different molecular weights: (a) $M = 342000$; (b) $M = 270000$; (c) $M = 220000$. The continuous parts of the curves at the high-concentration end are straight lines with slope 3.

Table I
Effective Length Parameters

MW	ϵ	concn, wt %	cL^3	cL_e^3
2.2×10^5	0.13	2.0	191	0.44
		6.0	598	1.37
		8.0	815	1.86
2.7×10^5	0.15	1.0	142.5	0.48
		3.0	436	1.47
		4.6	680	2.30
		6.6	996	3.36
		7.4	1127	3.80
		8.4	1293	4.36
3.4×10^5	0.13	1.5	327	0.67
		2.4	547	1.13
		3.6	824	1.70
		4.7	1097	2.26
		6.0	1420	2.93

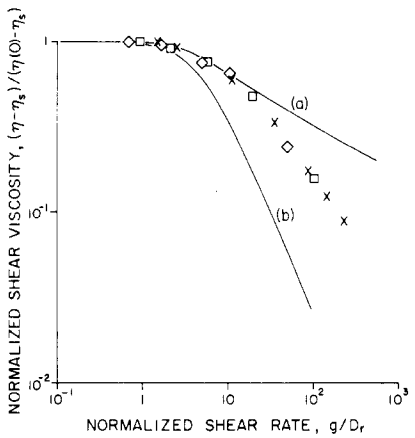

Figure 5. Comparison of experimental viscosity data with theoretical curve obtained from eq 9 using "best-fit" values of diffusion coefficients (horizontal shifts). Line a: extended theory; line b: original Doi-Edwards results. Experimental data from ref 5: (□) c = 3.0 wt %, D_r = 1.27 s^{-1}; (×) c = 4.6 wt %, D_r = 0.5 s^{-1}; (◇) c = 6.6 wt %, D_r = 0.15 s^{-1}.

highest concentrations below the liquid crystal transition.

Shear Rate Dependence of Viscosity. Figure 5 shows that the normalized shear viscosity $[(\eta - \eta_s)/(\eta(0) - \eta_s)]$ plotted vs. normalized shear rate, g/D_r, for three different concentrations of PBLG ($M = 2.75 \times 10^5$) in *m*-cresol examined by Hermans can be superposed on one another by choosing an appropriate value of the diffusion coefficient D_r (horizontal shift factor). At these concentrations and for the high value of β determined above, only eq 9 can lead to such a behavior and will thus be used without further justification. Figure 5 also shows the original prediction of Doi and Edwards, keeping only the dyadic term of the stress expression, and the new result, using the full eq 9. Although the new version of the theory overestimates the viscosity at high shear rate, it provides much better agreement with the experimental result up to γ = 20. The D_r values, chosen to "best fit" the theoretical curve, are plotted vs. cL^3 on a log-log scale in Figure 6 and follow a straight line of slope −2.16, which is in good agreement with the model which predicts a slope of −2. The value of β extracted from that curve is again of the order of 10^4, consistent with the value determined from the $\eta(0)$ calculations.

Kiss and Porter[6] have recently reported steady and oscillatory shear viscosities for PBLG ($M = 1.5 \times 10^5$) in *m*-cresol. The comparison of some of their steady shear viscosity data with the theoretical predictions are shown in Figure 7. The results are similar to the comparison of

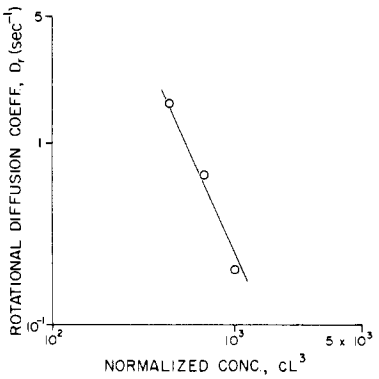

Figure 6. Plot of rotational diffusion coefficient obtained from Figure 5 vs. normalized concentration. The straight line has slope −2.16.

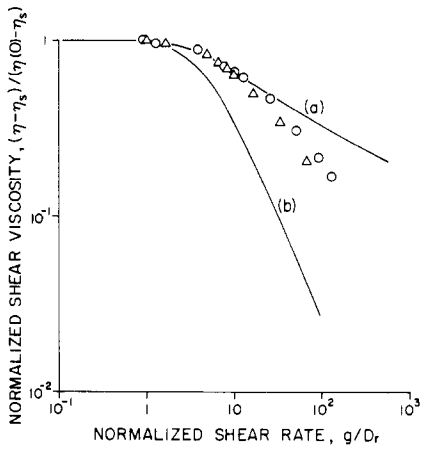

Figure 7. Comparison of experimental viscosity data with the theoretical prediction. Line a: extended theory; line b: original Doi-Edwards results. Experimental data from ref 6: (○) c = 6.1 wt %, D_r = 7.8 s^{-1}; (△) c = 7.5 wt %, D_r = 6.0 s^{-1}.

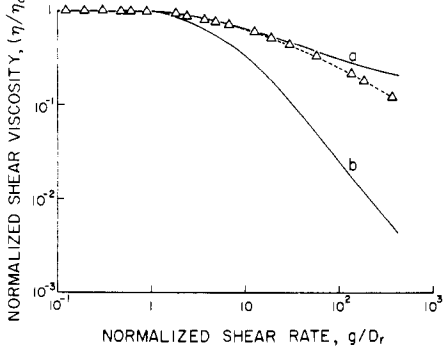

Figure 8. Comparison of the experimental master curve (- - -) obtained with several rodlike polymer solutions from ref 7 with curve of the extended theory (line a). The original Doi-Edwards results are represented by line b.

Hermans' data although the discrepancy at high shear rates is smaller in this case.

Figure 8 shows recent data taken by Berry and coworkers.[7] The data shown represent that of a 2.55% concentration of PBT ($M = 2.6 \times 10^4$) in a mixture of methanesulfonic acid and chlorosulfonic acid; the dashed experimental curve in Figure 8 truly represents a *master* curve of the normalized results of several rodlike polymer solutions of various concentrations and at various temperatures.[13] The agreement between these experimental results and the master curve of the extended model is gratifying, particularly in view of the fact that no fitting parameters were needed since the relaxation times (λ =

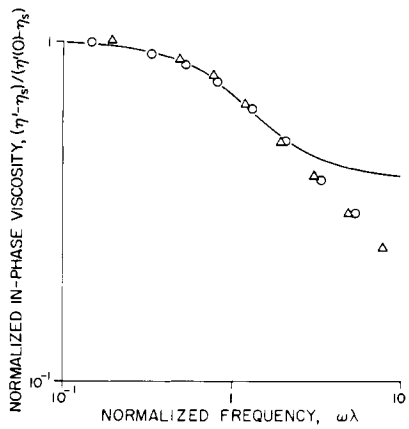

Figure 9. Comparison of experimental oscillating shear viscosity data with the theoretical prediction. Continuous line: theoretical curve. Experimental data from ref 6: (○) c = 6.1 wt %, D_r = 12.6 s^{-1}; (△) c = 7.5 wt %, D_r = 8.6 s^{-1}.

Table II
Steady Shear and Oscillatory Shear Results

concn, wt %	steady shear		oscillatory shear	
	D_r, s^{-1}	$\eta(0)$, P	D_r, s^{-1}	$\eta'(0)$, P
6.1	7.8	26.7	12.6	24.0
7.5	6.0	48.9	8.6	40.0

$1/6D_r$) were independently measured by Berry and coworkers. Compared to Berry's master curve, Kiss and Porter's viscosity data fall slightly below it at high shear rates, and those of Hermans still further below, making the comparison with the theoretically predicted curve poorer at high shear rates in Figures 5 and 7.

Frequency Dependence of Dynamic Viscosity. In Figure 9 we present the oscillatory shear viscosity data reported by Kiss and Porter[6] for the concentrations of 6.1 and 7.5% of PBLG in *m*-cresol also used in the steady viscosity measurements presented in Figure 7. Here again, the data for the two concentrations can be almost perfectly superposed on one another over the whole range of frequencies covered. Use of the stress expression in eq 9 leads to the following master curve relation for η':

$$\eta' - \eta_s = ckT\lambda\left[\frac{3}{5}\left(\frac{1}{1+(\lambda\omega)^2}\right)+\frac{2}{5}\right] \qquad (45)$$

which is also plotted in Figure 9 and compares very well with the experimental results up to $\omega\lambda \simeq 2.3$. This result is quite interesting since eq 45 is identical with the dilute-solution result[9] with the relaxation time λ properly accounted for.

In Table II we compare the parameters D_r obtained from the fitting of the steady shear results to those obtained from the oscillatory shear results. A slight discrepancy exists but should not be too worrisome in view of the fact that slight variations in D_r do not appreciably affect the comparison with the theory. Furthermore, we noted that the data of Kiss and Porter lead to slightly different values for the zero-shear viscosity $\eta(\gamma = 0)$ compared to those of the in-phase component $\eta'(\omega = 0)$ (see Table II). We note that $\eta(0)$ appears always to be slightly higher than $\eta'(0)$. This problem also exists in the case of dilute solutions, where, for example, the oscillatory shear data of a dilute solution of tobacco mosaic virus is well fitted to the theory of dilute solution with $[\eta'(0)] = 20$ cm^3/g[14] whereas literature values of $[\eta(0)]$ vary from 27 to 37 cm^3/g.[15] This discrepancy in viscosities would lead in the model to a discrepancy in D_r.

Discussion and Conclusion

The $\eta(0)$ vs. c^3 relationship predicted by the Doi and Edwards model is obeyed quite convincingly at the high-concentration end of the isotropic region and so is the D_r vs. c^{-2} relationship.[16] The value of the zero-shear-rate viscosity, $\eta(0)$, is, however, overestimated and accordingly the diffusion coefficient D_r is underestimated, as seen from the calculated magnitudes of the proportionality constant β. It is possible to interpret these results qualitatively by postulating that the "effective" length of the molecule in causing hindrance, L_e, is smaller than its physical length by a factor of about 6. It would then appear that the $\eta(0)$ vs. c^3 relationship holds experimentally in the isotropic concentration range for which $cL_e^3 \gtrsim 1.5$.

To evaluate the viscosity at high shear rates it was found necessary to include the fourth moment of orientation (quadrad term) in the stress expression. When the coefficient of that term is ckT/D_r rather than the originally proposed ckT/D_{r0}, agreement with experimental steady-state and in-phase oscillatory shear viscosity data is obtained over a reasonable range of shear rates and frequencies. Although D_r corresponds to the proper relaxation time in semidilute solutions, we have noted in the Introduction that there is yet no rigorous expression for the stress tensor of a semidilute solution of rigid rods.

The theory was developed for a monodisperse solution of infinitely thin rods. In comparing it with experimental results we have ignored the polydispersity of the samples. Berry's samples are fairly monodisperse with a polydispersity index of approximately 1.5.[13] Due consideration ought to be given to the molecular weight distribution and to the flexibility of the molecules before a more complete test of the theory can be made. Finally, apart from the neglect of hydrodynamic interactions, the translation–rotation coupling has also been ignored.

Turning to the assumption of infinitely thin rods, we note that the deviation of the kinetic equations (eq 4–6) implies that collisions between particles are dominated by the random Brownian motion rather than by the deterministic convective motion of the particles. Although this is correct in the limit of *infinitely* thin elongated rods, real particles are subjected to a convective motion in which each end describes an orbit whose period, T, has been calculated for ellipsoidal particles by Jeffery[17] to be

$$T = 4\pi/g(1-r^2)^{1/2} \qquad (46)$$

where

$$r = [1-(b/a)^2]/[1+(b/a)^2] \qquad (47)$$

with b and a being the minor and major axes of the ellipsoid, respectively. For eq 4–6 to hold for rods of finite thickness, the period for the molecule to execute a Jeffery orbit should be much larger than the rotational relaxation time; hence, T must satisfy

$$T \gg 1/D_r \qquad (48)$$

When $a \gg b$, eq 46–48 lead to

$$\frac{g}{D_r} \ll \frac{4(L/d)\pi}{\sqrt{2}} \qquad (49)$$

For a typical case of $L/d = 100$, we obtain

$$g/D_r \ll 900 \qquad (50)$$

which puts a high shear limit to the applicability of the model.

Within the above limitations, the model was shown to provide a good description of the rheological properties

examined here. From a practical point of view, the power of the model lies in the fact that it couples rheology and molecular orientation and thus provides means of estimating degrees of orientation dependent on flow conditions so important in polymer processes.

Acknowledgment. We thank Professor G. C. Berry for providing us with unpublished data on the shear viscosity of PBT solutions and several other communications. We also thank the Cornell Injection Molding Program group for encouragement and many useful discussions. This work was supported by NSF Grant DAR-7818868.

Appendix A. Derivation of Relationship between $\tilde{D}_r$, D_r, and D_{r0}

Consider a test rod with orientation $\vec{u}(t)$. Let its orientation at time $t = 0$ be $\vec{u}(0)$. Due to the hindrance by other rods it will remain within a solid angle $\Delta\Omega$ for a time of order τ_0, where τ_0 is the time in which the rod hindering the test rod will diffuse a distance L along its length. We can then write ($\sim$ stands for proportional to)

$$\tau_0 \sim L^2/D_{t0\|} \tag{A-1}$$

where $D_{t0\|}$ is the translational diffusion coefficient parallel to the axis of the rod given by Kirkwood's relation[12]

$$D_{t0\|} = kT \ln (L/d)/2\pi\eta_s L \tag{A-2}$$

with k being Boltzmann's constant and η_s being the solvent viscosity.

If a_c is the distance the test rod can move before colliding with another rod, then

$$\Delta\Omega = (a_c/L)^2 \tag{A-3}$$

The Brownian rotational diffusion of the test rod can hence be considered to be a random walk on a unit sphere with a jump frequency $1/\tau_0$ and a mean-square displacement $(a_c/L)^2$. Therefore, D_r is given by

$$D_r \sim (a_c/L)^2/\tau_0 \tag{A-4}$$

The determination of a_c proceeds as follows: consider a cylinder of radius a enveloping the test rod. Let $N(a)$ be the mean number of rods penetrating this cylinder. The value of a_c is determined by setting

$$N(a_c) = 1 \tag{A-5}$$

To obtain $N(a)$, let dS be a surface element on the cylinder of radius a enveloping the test rod and $\vec{v}$ be the vector normal to dS. If $\vec{u}'$ is the orientation of the penetrating rod, then

$$dN = cL\, dS \int d^2\vec{u}' |\cos(\vec{v}\vec{u}')| f(\vec{u}') \tag{A-6}$$

where dN is the number of rods penetrating the area dS. The notation $\cos(\vec{v}\vec{u}')$ means the cosine of the angle between vectors $\vec{v}$ and $\vec{u}'$.

Integrating (A-6) over the whole surface of the cylinder gives

$$\int dN = cL \int dS \int d^2\vec{u}' |\cos(\vec{v}\vec{u}')| f(\vec{u}') \tag{A-7}$$

However, since $a \ll L$, most of the rods penetrate the cylinder twice, and therefore

$$\begin{aligned} N(a) &= \tfrac{1}{2}cL \int dS \int d^2\vec{u}' |\cos(\vec{v}\vec{u}')| f(\vec{u}') \\ &= \tfrac{1}{2}caL^2 \int d^2\vec{u}' f(\vec{u}') \int_0^{2\pi} \sin(\vec{u}\vec{u}') |\cos\theta|\, d\theta \\ &= 2caL^2 \int d^2\vec{u}' \sin(\vec{u}\vec{u}') f(\vec{u}') \end{aligned} \tag{A-8}$$

Since at equilibrium

$$f(u') = 1/4\pi \tag{A-9}$$

we find

$$N_{eq}(a) = (\pi/2)acL^2 \tag{A-10}$$

Use of (A-5) leads to

$$a_{c,eq} = (2/\pi)(1/cL^2) \tag{A-11}$$

On the other hand, we have the relation[12]

$$D_{r0} = kT \ln (L/d)/3\pi\eta_s L^3 \tag{A-12}$$

Using (A-1), (A-4), (A-11), and (A-12) yields

$$D_r \sim D_{r0}(cL^3)^{-2} \tag{A-13}$$

or

$$D_r = \beta(cL^3)^{-2} D_{r0} = \beta(\pi a_{c,eq}/2L)^2 D_{r0} \tag{A-14}$$

Under flow conditions, we have from (A-8)

$$a_c^{-1} = 2cL^2 \int d^2\vec{u}' \sin(\vec{u}\vec{u}') f(\vec{u}')$$

and therefore we get

$$\tilde{D}_r(\vec{u},[f]) = D_r\left[(4/\pi) \int d^2\vec{u}' f(\vec{u}',t) \sin(\vec{u}\vec{u}')\right]^{-2} \tag{A-15}$$

where we have made use of (A-14).

References and Notes

(1) Doi, M.; Edwards, S. F. *J. Chem. Soc., Faraday Trans 2* **1978**, *74*, 560, 918.
(2) Bird, R. B.; Hassager, O.; Armstrong, R. C.; Curtiss, C. F. "Dynamics of Polymeric Liquids"; Wiley: New York, 1977; Vol. 2, p 530, eq 11.3-2.
(3) Reference 2, p 537.
(4) Riseman, J.; Kirkwood, J. G. *J. Chem. Phys.* **1950**, *18*, 512.
(5) Hermans, J., Jr. *J. Colloid Sci.* **1962**, *17*, 638.
(6) Kiss, G. K.; Porter, R. S. *J. Polym. Sci., Polym. Phys. Ed.* **1980**, *18*, 361-88.
(7) Unpublished data of G. C. Berry and co-workers.
(8) Curtiss, C. F.; Bird, R. B. *J. Chem. Phys.* **1981**, *74*, 2016, 2026.
(9) Kirkwood, J. G.; Plock, R. J. *J. Chem. Phys.* **1956**, *24*, 665.
(10) Doty, P.; Bradbury, J. H.; Holtzer, A. M. *J. Am. Chem. Soc.* **1956**, *78*, 947.
(11) The same order of magnitude of β is obtained if eq 8 is used.
(12) See: Kirkwood, J. G.; Auer, P. L. *J. Chem. Phys.* **1951**, *19*, 281.
(13) Berry, G. C., private communication.
(14) Reference 2, p 540.
(15) Nemoto, N.; Schrag, J. L.; Ferry, J. D.; Fulton, R. W. *Biopolymers* **1975**, *14*, 407-17.
(16) Maguire, J. F.; McTague, J. P.; Rondelez, F. *Phys. Rev. Lett.* **1980**, *45*, 1891.
(17) Jeffery, G. B. *Proc. R. Soc. London, Ser. A* **1922**, *102*, 161.